

# TAPHONOMY OF THE EOCENE LONDON CLAY BIOTA

by PETER A. ALLISON

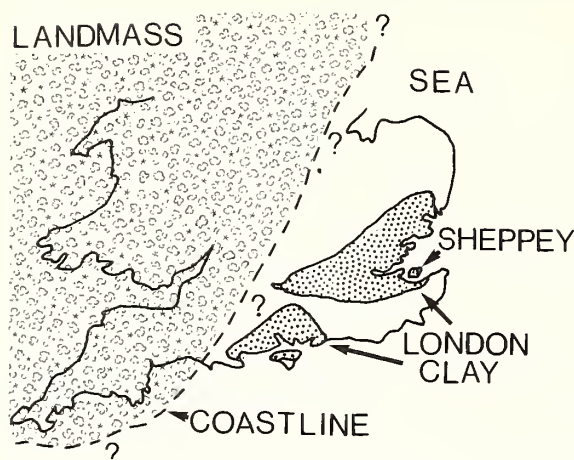
**ABSTRACT.** The London Clay of Sheppey, Kent, is a grey plastic clay which was deposited in an offshore marine environment. It contains a diverse assemblage of well-preserved plant and animal fossils in concretions of either pyrite, apatite, or calcite. A diagenetic and geochemical study of the London Clay biota shows that apatite was the first preservational mineral to form, followed by calcite and pyrite. Mineralogy is strongly related to original biological composition. Only those organisms with an original skeletal phosphate content (i.e. vertebrates and arthropods) have been phosphatized. Thus a geochemical bias accounts for the preservation of the greatest detail in fossils of these groups. Early diagenetic mineralization is the only process which can halt the information loss occurring during decay. For this reason organisms preserved during the earliest phases of mineralization retain the most detail.

THE organic precursors of fossils can be thought of as chemically exotic sedimentary particles which achieve equilibrium with the surrounding sediment by decay and mineralization. Details of the nature and mineralogy of preservation can therefore yield information on the diagenetic and geochemical history of the enclosing strata. In addition, a fuller understanding of the processes responsible for early diagenesis and exceptional preservation will pin-point possible locations for new exceptionally preserved biotas.

Allison (1988a) has shown that anoxia is ineffective as a long-term preservational medium and that only mineralization can halt decay-induced information loss in the fossil record. Further, preservational mineralogy of a biota is strongly related to original organic composition. This results in a geochemical taphonomic bias whereby those fossils associated with the earliest phases of mineralization exhibit a higher level of preservation than those formed by later events.

The London Clay biota presents a variety of exceptionally preserved plant and animal remains and can be defined according to Seilacher (1970; see also Seilacher *et al.* 1985) as a *Konservat* or conservation *Lagerstätten*. This study examines the mineralogy and preservation of the London Clay biota and discusses the palaeoenvironment and diagenetic sequence of the host rock. The London Clay flora represents one of the world's most diverse fossil fruit and seed assemblages, containing over 500 plant types including 300 named species (Collinson 1983). It is regarded as one of the best preserved and most diverse assemblages of fossil plant material in Europe. For a taxonomic review of the flora, see Chandler (1961, 1964) and Collinson (1983).

The animals of the London Clay biota are as well preserved as the plants. The hard parts of mammals, birds, reptiles, fish, arthropods, and molluscs almost always occur in three dimensions within pyrite or calcium phosphate concretions. Soft-part preservation is very scarce, but includes a pyritized maggot (Rundle and Cooper 1970) and the pedicle of a terebratulid brachiopod (Rowell and Rundle 1967). The diversity of the fauna has attracted considerable scientific attention from invertebrate and vertebrate specialists alike, e.g. Murray and Wright (1974) on the Foraminifera, King and King (1976) on the brachiopods, Davis and Elliott (1957) and Curry (1965) on the molluscs, Keen (1978) on the ostracodes, Quayle and Collins (1981) on the crabs and lobsters, Casier (1966) and Ward (1979) on some of the fish, and Hooker *et al.* (1980) on some of the mammals and reptiles.



TEXT-FIG. 1. Map showing palaeogeography of southern Britain during Eocene times. Principal occurrences of London Clay are arrowed.

### GEOLOGICAL SETTING

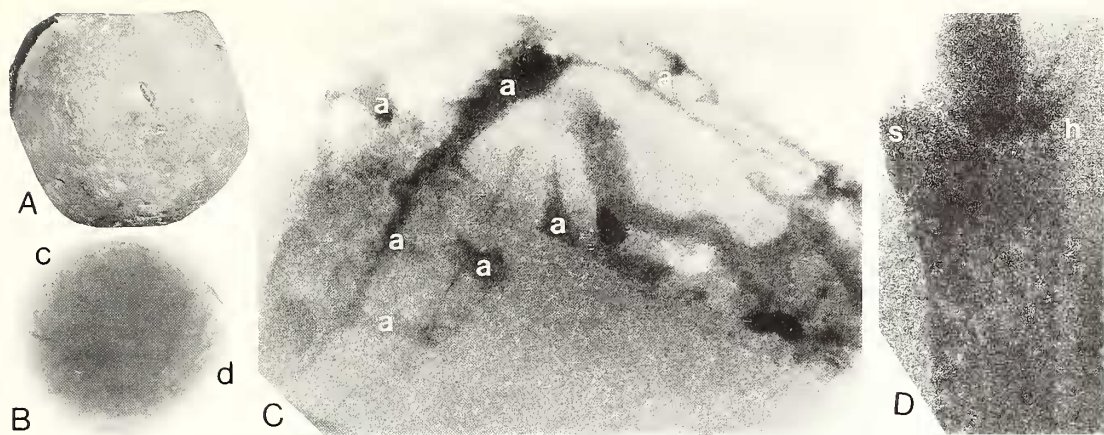
Outcrop of the London Clay in the British Isles is limited to the London and Hampshire basins (text-fig. 1). By far the best and most complete sections occur along the coast, although brick pits and motorway cuttings have created additional exposure (see Collinson 1983 for details). Although these basins are currently separated by the Chalk ridges of the Downs, they were originally deposited in a single trough along the northern flank of the Anglo-Paris Basin (Curry 1965; Davis and Elliot 1957; Wills 1951). Repeated subsidence and sedimentation has resulted in a cyclic sequence of marine, brackish, and estuarine deposits. The clay mineral suite occurring in Tertiary sediments from the western part of the Hampshire Basin is dominated by a kaolin-illite assemblage derived from the West Country granites (Gilkes 1967). However, the sediments occurring in the east are rich in montmorillonite and may be derived from either locally eroded Chalk (Gilkes 1967) or the decomposition of pyroclastic ash deposits (Knox and Harland 1979). During marine transgressions of the basin, such as that responsible for the deposition of the London Clay, the illite/montmorillonite suite extended from the eastern province to include both the London and Hampshire basins. The shore line during London Clay times is thought to have run south-west roughly from the Wash to a few miles west of the Isle of Wight (text-fig. 1; Wills 1951). Sand and silt horizons occurring near what was the Eocene shoreline thin eastwards (King 1981) into the stiff blue-grey muds which are so characteristic of the London Clay.

The London Clay within the London Basin attains its maximum thickness of 165 m on the Isle of Sheppey where it crops out as a series of monotonous stiff blue-grey clays with numerous nodule bands (Davis 1936). King (1981) proposed a lithostratigraphical classification of the London Clay and the associated beds, which together he referred to as the Thames Group. In his classification this group is divided into the Oldhaven and London Clay formations. The latter is further sub-divided into divisions A-E of which the upper two (D and E) crop out along the Sheppey coast.

By far the best exposed section at Sheppey occurs at Warden Point where almost 50 m of sediment are exposed. Much of the material upon which this study is based was collected from either the pyrite and nodule concentrates on the foreshore or *in situ* from the cliff.

### PRESERVATIONAL STYLE

*Vertebrates.* At Sheppey fish teeth and vertebrae are the most common vertebrates, although mammalian (Hooker *et al.* 1980) and avian remains have been recorded (Harrison and Walker 1977). The fossils are most commonly preserved in concretions of either phosphate or pyrite and seldom occur in carbonate concretions. Phosphatic fossils show a greater degree of articulation and in some cases may be completely intact. Preservation of some of the fish includes articulated hard parts (skull, vertebrae, etc.) enclosed by a cylindrical bag of scales in what appears to be life position. Soft parts (muscles and viscera, etc.) are absent from such fossils and the scales are



TEXT-FIG. 2. A, phosphatic crab-bearing concretions,  $\times 0.8$ . B, X-ray radiographic print of concretion showing partially disarticulated crab; c and d refer to areas of X-ray enlarged in text-fig. 2C, D,  $\times 0.8$ . C, D, photographic enlargements of B. C shows crab pincer with apodemes (a),  $\times 7$ . D, crab leg with spine (s) and possible skirt of sensory hair (h),  $\times 10$ . X-ray photographs were taken with a PHILLIPS MG 161-160 kV constant potential X-ray unit. The X-ray tube had a focus of  $0.4 \times 0.4$  mm and a film focus distance of 600 mm. Inherent filtration of the X-ray tube was equivalent to 1 mm of beryllium.

separated from the skeleton by phosphatized sediment. Thus it is clear that decay had destroyed soft tissues prior to phosphatization. Decay of soft parts commonly leads to tissue collapse and flattening of carcasses (Zangerl and Richardson 1963; Zangerl 1971; Conway Morris 1979; Briggs and Williams 1981). The preservation of scales in an uncompacted life position therefore implies that sediment infill of the body cavity occurred during the decay of soft parts. Such a mode of preservation could only be achieved with extremely rapid rates of sedimentation.

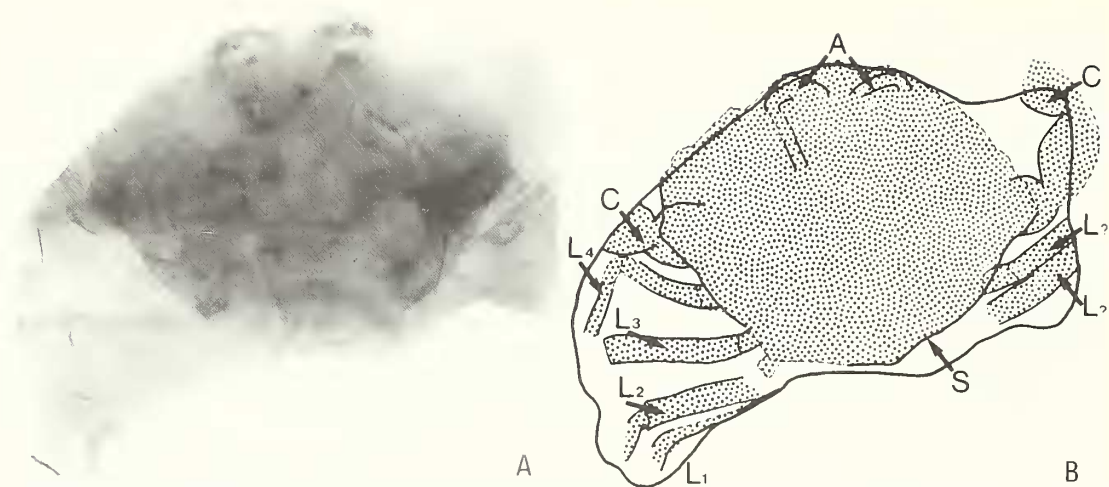
Vertebrate hard parts within these concretions are preserved in brown-black calcium phosphate in contrast to the buff colour of the enclosing concretion.

*Arthropods.* The arthropod fauna is dominated by crabs and lobsters although barnacles and insects also occur. Insects are pyritized and three-dimensional, and include both adult and larval forms (Venables and Taylor 1963). Rundle and Cooper (1970) suggested that the insects at Sheppey were wood-boring forms which may have been transported in floating timber.

Eumalacostracans are always preserved in dark francolite within buff-coloured concretions of calcium phosphate (text-fig. 2A). They are invariably fragmented and disarticulated but are rarely flattened and show fine morphological detail including cuticle lamination and pore canals (text-fig. 6I). In some specimens it is possible to differentiate between endo- and exocuticle (text-fig. 6I). X-ray radiographic methods have demonstrated the preservation of delicate structures such as spines, sensory hairs (text-fig. 2B, D), the antennae of a crab (text-fig. 3A, B), and even the apodemes or muscle attachment sites on the inside of a crab pincer (text-fig. 2C).

X-ray methods have usually been used in the past to detect pyritized structures. The phosphate in which the London Clay arthropods are preserved is chemically similar to that of the enclosing nodule. However, the phosphate of the crustacean cuticle is more densely crystalline than the enclosing phosphatized sediment. Thus, the fossils are only rendered visible to X-rays by a slight difference in density/porosity between the calcium phosphate of the concretion and that of the arthropod cuticle. Flattened concretions are more amenable to X-rays than rounded forms. This is because variations in thickness in the concretion affect the absorbance of X-rays and thereby control the exposure of the radiograph. Thus flattened concretions with an even thickness have a uniform exposure (text-fig. 3A). Rounded concretions present a technical problem in that very few





TEXT-FIG. 3. A, X-ray radiographic print of crab in phosphate concretion,  $\times 1.6$ . B, drawing of X-rayed specimen, L = appendages, S = carapace, A = antennae, C = pincers.

X-rays pass through the thicker centre of the concretion compared with the thinner periphery. Prints taken from such radiographs of the periphery of the concretion require considerable photographic 'dodging'. In the case of the print showing the crab chelae (text-fig. 2c) the upper margin of the print received 360 times as much light as the lower margin of the print.

*Shelly fossils.* Molluscs and brachiopods are commonly found as isolated elements amongst pyrite concentrates on the beach at Sheppey. They are commonly infilled with pyritized sediment and/or euhedral pyrite. Pyrite often replaces original shell, although even where this is the case, it is possible to pick out original laminar skeletal structure. In some cases it is possible to identify vertical rods of pyrite normal to the shell surface which appear to be pseudomorphing original skeletal fabric (text-fig. 6D). Calcareous relics of the original shell are rare within these pyritized remains but occasionally the more heavily calcified parts, such as the spire of gastropods survive (text-fig. 6E, G). Original shell material of both gastropods and bivalves is found in concretions of calcium carbonate (text-fig. 4) and calcium phosphate. In this instance even delicate shells are uncracked and show no indication of sediment compaction. Concretion formation was therefore pre-compactional.

Borings of the bivalve *Teredina squamosa* are common in calcified (text-fig. 4) and pyritized (text-fig. 9E) wood within concretions. Modern representatives of *Teredina* have a reduced shell which is rocked back and forth by the animal as it bores its way into the wood. Since most of the soft parts lie outside the shell, the animal secretes a thin layer of calcite to line the boring. Within calcified wood from Sheppey this lining calcite is ubiquitous, and the articulated shells are found in the boring. Tangential sectioning of mineralized borings reveals a series of semi-vertical striations running along the edge (text-fig. 5D) which were made by the rocking motion of the shell. Some of the borings contain irregular spherical bodies of dark brown calcite up to 6 mm in diameter (text-fig. 5A). These may be the calcified gastric contents left in their original location following decomposition of the soft parts.

*Plants.* The plants demonstrate a greater preservational diversity than the animals (see Table 1).

*Coalified plant matter.* The cuticles of pyritized fruits and seeds may be preserved as coalified remnants. In addition, isolated woody fragments occur throughout the clay which are part

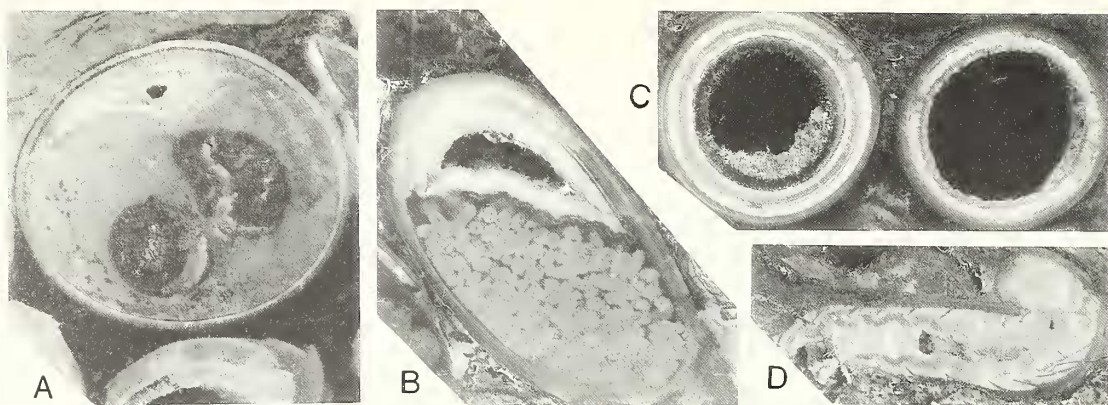




TEXT-FIG. 4. Transverse section of wood-bearing concretion,  $\times 0.8$ . Note extensive boring by bivalve *Teredina*: s = gastropod shell, m = pyrite meniscus, l = shell lag, t = burrow, g = geopetal infill with pellets/sediment, z = polyzonal-calcite lining *Teredina* boring.

TABLE 1. Summary of mineralogical facies associated with fossilization in the London Clay.

	Pyrite	Calcium carbonate	Calcium phosphate
Framboids	a, Isolated b, Conjoined		
Fossils	a, Plants: fruits and wood b, Shelly material c, Vertebrates	a, Original skeletal material b, Permineralized wood	a, Arthropods and vertebrates b, Permineralized seed cases
Internal moulds	a, Vessel infills in calcified wood b, Vesicle infills in bone c, Cavity infills in gastropods and <i>Teredina</i> borings. Includes: pyritized sediment, euhedral pore lining pyrite, and pyrite stalactites	a, Cavity infills with pore lining habit in <i>Teredina</i> borings	a, Mineralized sediment infill of cavities in seeds
Overgrowths	a, Burrow infills b, Bi-pyramidal forming: light 'dustings' and cauliform growths c, Radiating cauliform growths		
Concretions	a, Sub-spherical to flat and cauliform	a, Sub-spherical to ovate concretions	a, Sub-spherical to ovate nodules
Septarian infills	a, In phosphatic nodules b, In pyritic nodules	a, In calcareous nodules	



TEXT-FIG. 5. A, dark-brown calcareous concretions, supposed to be gastric contents of *Teredina*, deposited *in situ* through decay of animal,  $\times 4$ . B, gcopetal pelletal infill of boring,  $\times 5$ . C, bore-lining polyzonal calcite,  $\times 5$ . D, tangential longitudinal section of boring showing striations upon wood surface made during excavation,  $\times 3$ .

pyritized and part coalified (text-fig. 6A). Unmineralized coalified material is always compacted and cellular detail is usually obscured.

**Pyritization.** Pyrite has preserved fine morphological details such as winged seeds inside a fruit (Collinson 1983) and cellular structure such as the cast and moulds of starch grains within mangrove hypocotyls (Wilkinson 1983). Robust structures such as twigs and seeds have not been crushed by sediment overburden but some of the fruits have been compacted. Thus the seed case of the large palm fruit *Nipa burtini* is compacted and slightly flattened (Pl. 94, figs. 1, 3, 5). Pyrite is most common as an infilling of cellular cavities but also occurs as a replacement of original plant material.

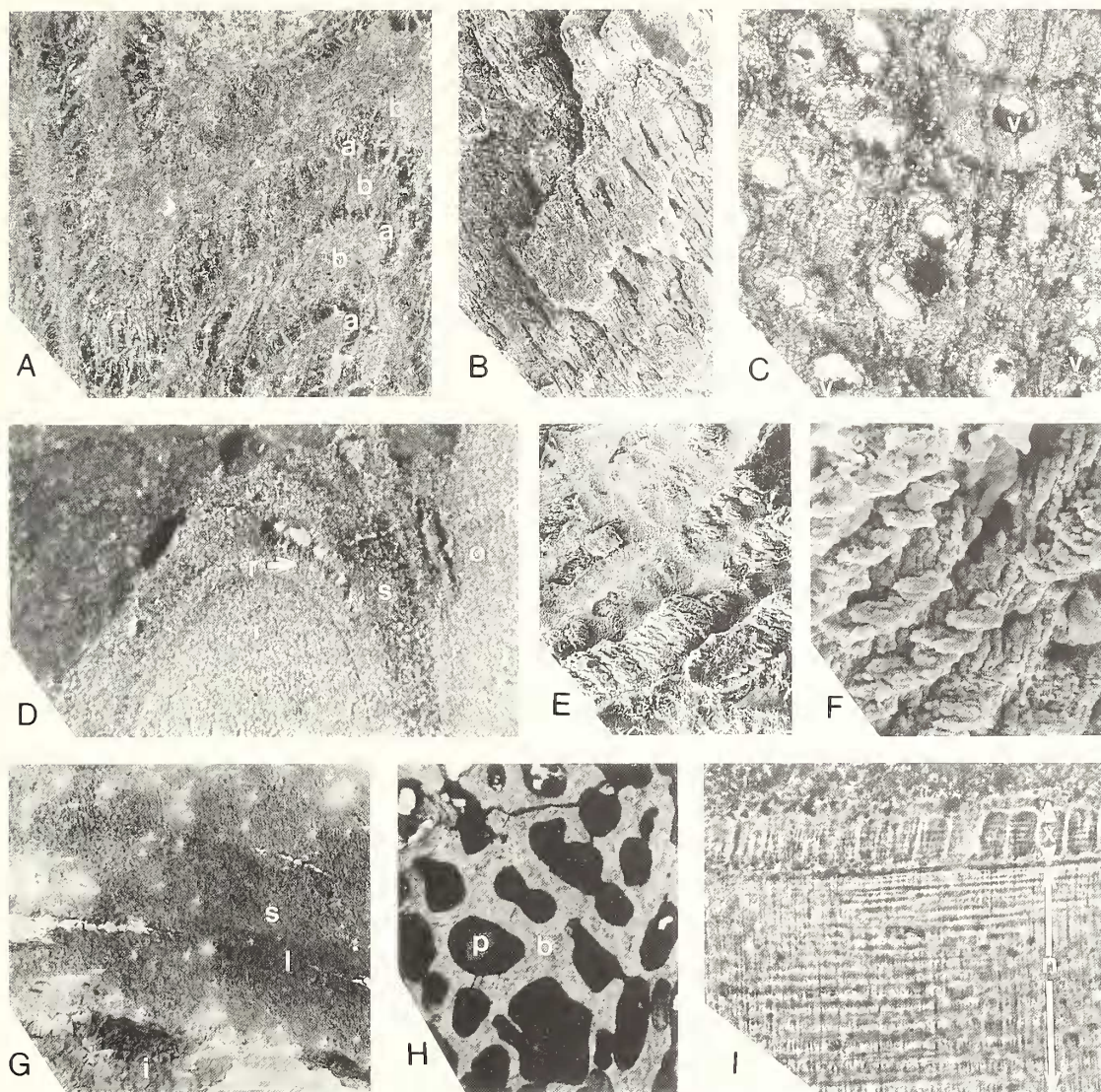
The development of pyrite is controlled by the anatomy of the original organic material. Mineralization preferentially selects the spring or early wood leaving the late or summer wood as a coalified layer (text-fig. 6A) with infillings of pyrite. Pyrite forms as a response to the activity of sulphate-reducing bacteria (see section on pyrite paragenesis). It is possible that the large, thin-walled cells of the spring wood were more susceptible to decay (by sulphate-reducing bacteria) than the small, thick-walled lignified cells of the late wood. Thus in the case of the wood figured in text-fig. 6A, the action of microbial sulphate reducers led to the decay of spring wood prior to the precipitation of pyrite. However, the late wood being more decay resistant, was preserved as a coalified residue which includes cellular detail. Individual cells in this instance are commonly infilled with pyrite. Similarly the tough outer cuticle of fruits such as *Nipa* is carbonaceous whilst the internal structures are pyritized. It is likely that this too is due to increased decay resistance within the cuticle.

Kenrick and Edwards (1988) have described a similar distribution of pyritized and coalified portions of plant anatomy from the Lower Devonian of Wales.

**Calcification.** Calcification of plant material occurs as a permineralization (as opposed to a replacement) and is restricted to larger woody fragments which have in some cases formed the nuclei of large carbonate concretions. Calcification led to the preservation of fluid-bearing vessels and individual cells (text-fig. 6B, C).

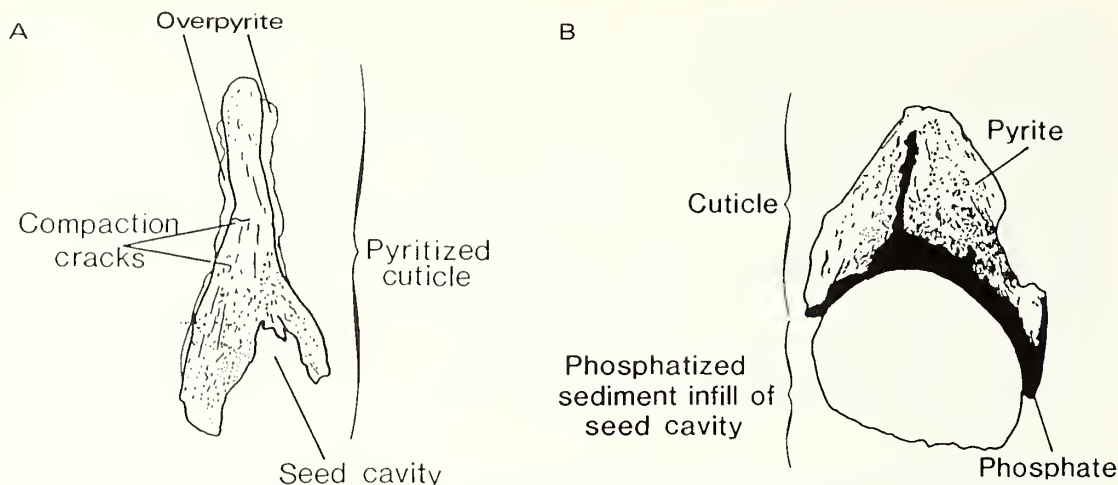
**Phosphatization.** Phosphatized plant material is rare and restricted to a few isolated specimens of *N. burtini*. The phosphate has impregnated the carbonaceous outer cuticle of the fruit and also occurs as a mineralized sediment infill within the fruit cavity (Pl. 94, figs. 2, 4, 6). *Nipa* from





TEXT-FIG. 6. A, pyritized wood cut perpendicular to grain and viewed in reflected light, note preservation of late wood (a) as coalified residue and early wood (b) as pyrite,  $\times 5$ . B, SEM of calcified wood,  $\times 20$ . C, thin-section of calcified wood showing cellular structure and fluid-bearing vessels (v), note geopetal infill of latter with framboidal pyrite,  $\times 30$ . D, pyritized gastropod shell (s) coated in overpyrite (o) with internal cavity filled with pyritized sediment (i), note vertical rods (r) of pyrite thought to represent original shell structure, viewed in reflected light,  $\times 20$ . E, SEM of calcareous spire of otherwise pyritized gastropod,  $\times 1200$ . F, close-up of E showing fine detail of lamellae structure of shell,  $\times 2000$ . G, SEM of pyritized gastropod shell (s) showing shell laminae (l), and pyritized sediment infill (i),  $\times 30$ . H, thin-section of phosphatized bone (b) with pyrite infill (p) of vesicles,  $\times 40$ . I, thin-section of phosphatized crab cuticle including preservation of exo-cuticle (x) and endo-cuticle (n)  $\times 35$ .





TEXT-FIG. 7. Diagram of polished sections of *Nipa burtini*. A, pyritized crushed specimen (Pl. 94, fig. 5). B, phosphatized/pyritized specimen (Pl. 94, fig. 6).

Sheppey displays considerable biological variation. Some forms are sterile and without fruit, others have been fertilized and have aborted and still others are fertile fruit-bearing forms (M. E. Collinson, pers. comm.). It is therefore important to identify the nature of each specimen and compare like with like before interpreting the effects and timing of compaction. The *Nipa* depicted in Plate 94, figs. 1, 3, and 5 is pyritized and is slightly flattened with compaction cracks (text-fig. 8) whereas the specimen depicted in Plate 94, figs. 2, 4, and 6 is part phosphatized/part pyritized and is three-dimensional (text-fig. 7). Phosphatization prevented flattening of the fruits and is therefore pre-compactional whereas pyritization occurred later after sediment overburden had crushed the fruits. It is possible that the pyrite occurring with phosphate in the uncompacted fruits is a replacement of original phosphate.

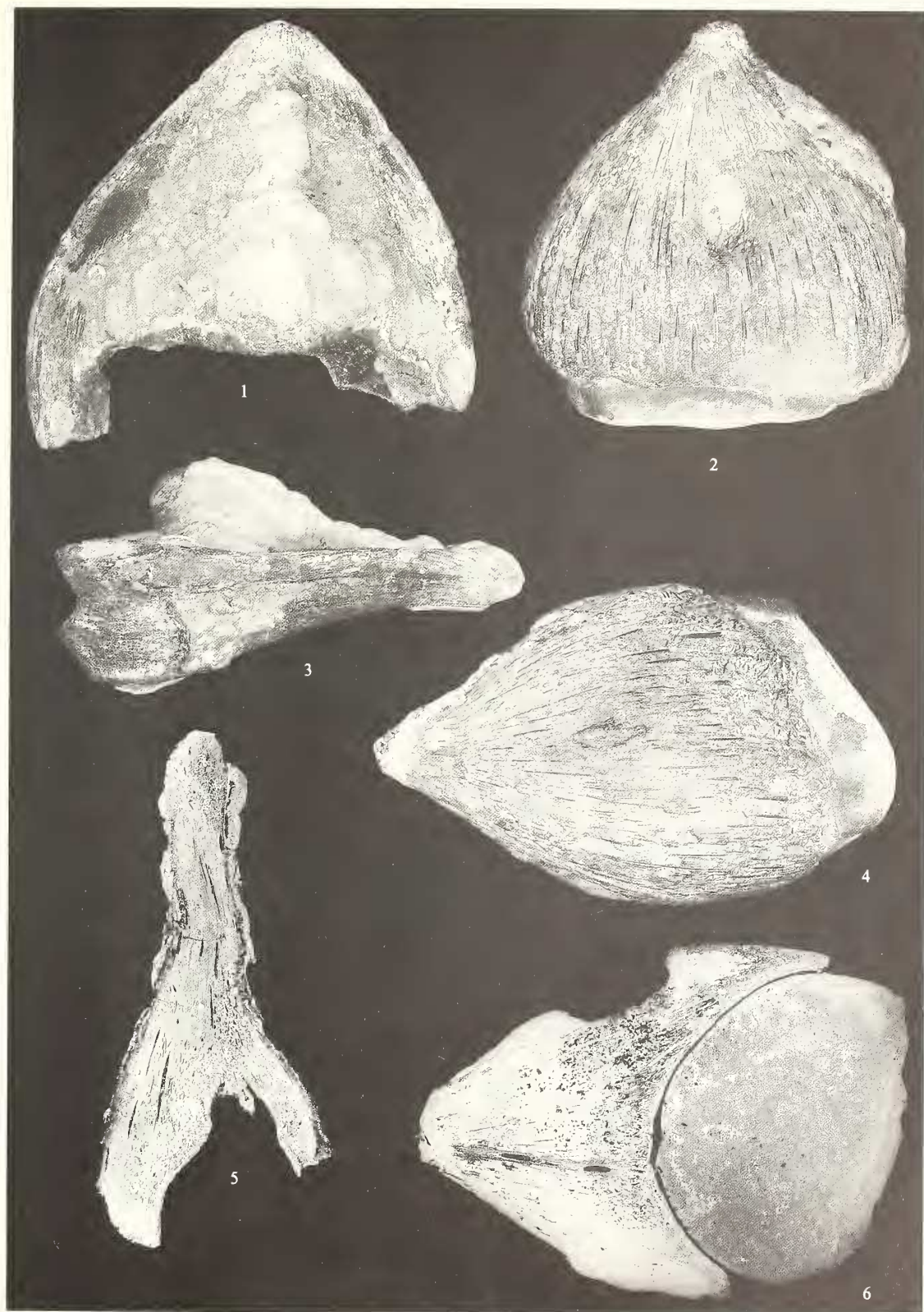
#### PRESERVATIONAL MINERALOGY

Most of the early diagenetic authigenic minerals are precipitated as a result of the biodegradation of organic matter. This is due to changes in Eh, pH, and in the concentration of various anionic and cationic species within pore waters brought about by bacterial respiration. Bacterial degradation proceeds through a number of chemical steps of which the best known is aerobic decay. However, following the depletion of oxygen, bacteria utilize a number of alternative oxidizing agents to continue active biodegradation and respiration. These reactions are stratified within sediment (text-fig. 8). Species liberating the greatest free energy yield occur highest in the sequence and only when these have been exhausted do less energetic reactions (lower in the column) occur (Redfield 1958).

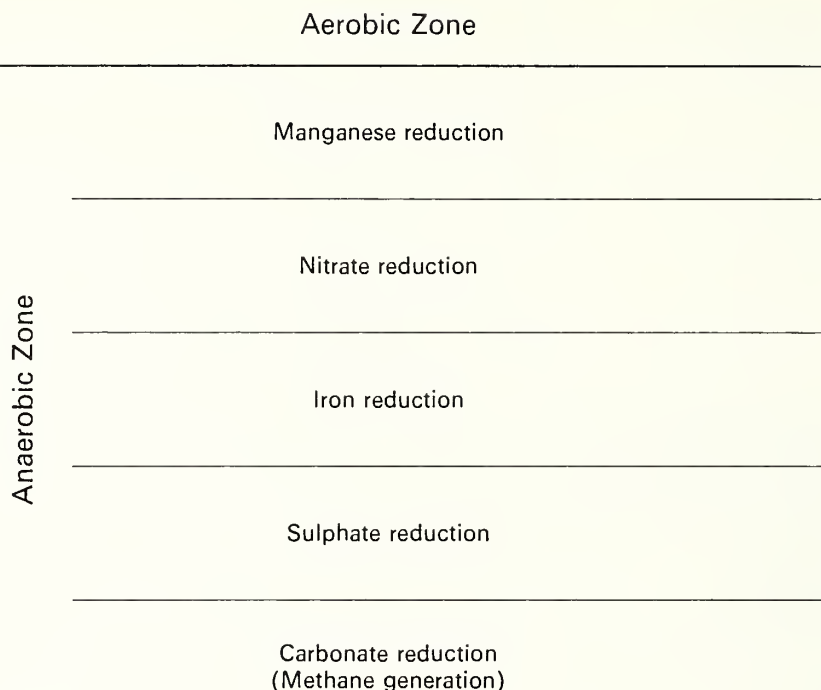
Not all oxidants are present within any given sediment. Sulphate reduction and methanogenesis dominate in marine environments whilst methanogenesis alone dominates in a freshwater system.

#### EXPLANATION OF PLATE 94

Figs. 1–6. *Nipa burtini*. 1, 3 and 5, apex of crushed pyritized specimen. 1, outline view. 3, lateral view. 5, polished section. 2, 4 and 6, apex of uncrushed phosphatized/pyritized specimen. 2, outline view. 4, lateral view. 6, polished section, all  $\times 2.6$ .



ALLISON, *Nipa burtini*



TEXT-FIG. 8. Occurrence of bacterial reduction zones in sediment (after Redfield 1958). Note sulphate reduction dominates in a marine system and methanogenesis and nitrate reduction dominates in a freshwater system (from Allison 1988a).

The sequence of decomposition events will have a radical effect upon pore-water chemistry and can therefore be used as a model for the paragenesis of several authigenic sedimentary minerals (text-fig. 8; see Berner 1981 for a review).

*Rationale.* Concretionary calcite and phosphate precipitate within the pore spaces of the unconsolidated clay. Crystallization of these minerals did not force the detrital minerals apart since delicate structures such as burrows and faecal pellets are still intact and undeformed. Thus the volume of nodule-forming mineral is approximately equal to original porosity of the sediment at the time of mineral precipitation (Raiswell 1971). Sediment compaction in mud rocks is proportional to depth of burial (Greensmith 1978), hence an assessment of original porosity within early cemented mud rocks is also an indication of diagenetic timing. Therefore original porosity of the sediment is approximately equivalent to the acid soluble fraction of the concretions (Raiswell 1971). This approach is invalid for pyrite and phosphate concretions since the acids capable of digesting these minerals will also dissolve detrital minerals such as some clays. For this reason calcium and phosphate levels in the apatite concretions was determined analytically and volume of nodule-forming mineral estimated. Even this method would be invalid for pyrite concretions since pyrite may replace detrital grains.

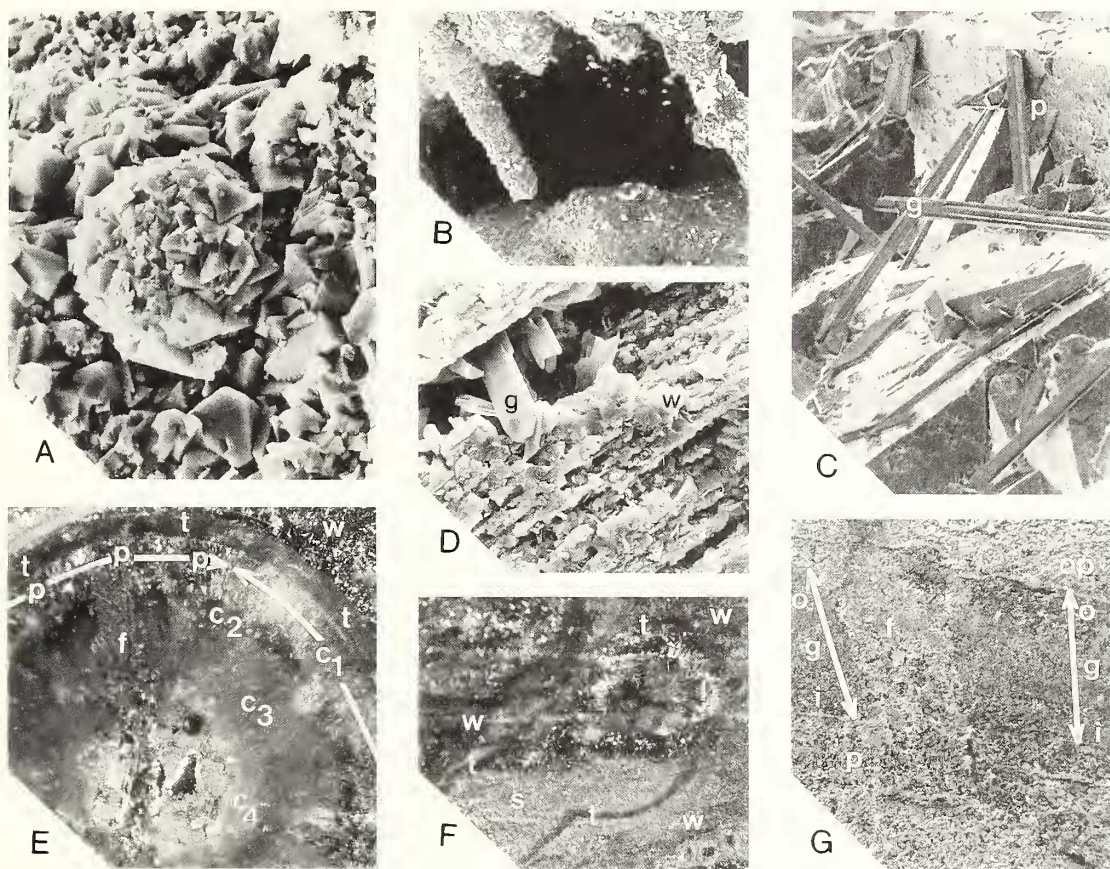
Minor and trace element chemistry of diagenetic minerals is strongly dependent upon pore-water chemistry at the time of crystal growth. Pore-water chemistry is in turn controlled by bacterial degradation of organic carbon and burial. Therefore the relative abundances of certain elements (particularly manganese) within the concretion can be analysed to provide an indication of diagenetic trends.



**Sampling.** Sampling for original porosity determination and chemical analysis was achieved by taking a thin slice of rock from the centre of a nodule and cutting it to produce a square sectioned core. This was then cut into cubes to allow porosity determination and chemical analysis of different parts of the concretion. Analysis was undertaken by atomic absorption spectroscopy using a Pye UNICAM PU 9000 instrument with aqueous solutions prepared from the calcareous and phosphatic samples. Phosphate analysis was achieved by colour density spectrophotometry using a Phillips SP 38 Spectrophotometer.

### Pyrite

**Morphology.** Pyrite exhibits a variety of morphological types (Hudson 1982). Studies of the morphologies and occurrences of pyrite in the London Clay allow the different phases of its



TEXT-FIG. 9. A, unusual framboid of octahedral pyrite upon surface of calcified/pyritized wood,  $\times 600$ . B, pyrite stalactites in gastropod cavity,  $\times 50$ . C, coarse cubic overpyrite (c) with slender crystals of gypsum (g) as alteration product,  $\times 80$ . D, calcified and pyritized wood (w) with prominent gypsum crystals (g),  $\times 20$ . E, pyritized wood (w) with *Teredina*-boring viewed in reflected light, note infill of boring with original *Teredina* calcite (t) and four coloured bands of authigenic calcite (C<sub>1</sub>-C<sub>4</sub>); pyritization (p) of authigenic calcite is limited to the outer (C<sub>1</sub>) zone, all four zones of calcite are cut by pyrite-filled fracture (f),  $\times 20$ . F, pyritized wood (w) with *Teredina* boring lined with *Teredina* calcite (t) and infilled with geopetal pyritized sediment (s) and cavity-lining pyrite (l),  $\times 20$ . G, gastropod shell (g, outer margin = o and inner margin = i), note that pyrite-infilled compaction fracture (f) is contiguous with overpyrite (op) and cavity-lining (p),  $\times 30$ .

formation to be dated in relation to the formation of early diagenetic calcium carbonate and calcium phosphate.

1. Isolated and conjoined framboids are randomly dispersed in concretions and the host sediment. Individual framboids range between 10–100  $\mu\text{m}$  in diameter (text-fig. 9A). Conjoined framboids occur as either linear or clustered aggregates: in the former as few as four framboidal crystallites are joined in a single plane, whereas the latter consists of a large number of framboids which have coalesced in a sub-spherical 'clot'. The linear forms are always parallel or sub-parallel and appear to delineate original sediment lamination. In some cases the 'clots' form thin coatings upon fossils. The framboidal-pyrite replacement of wood shown in text-fig. 4 for example, occurs as a 1 mm surface layer. This pyrite layer is limited to what would have been a hollow on the surface of the wood below a shell lag horizon. Such a 'meniscus' development of pyrite may be due to the development of a localized anoxic micro-environment within a topographic hollow.

2. Pyritized fossils are concentrated by wave action as lag deposits on the modern beach. Pyrite in plant material occurs as octahedral crystals approximately 10–20  $\mu\text{m}$  in size (text-fig. 6A). Where original shell material of molluscs and brachiopods has been pyritized the individual crystallites adopt a bipyramidal form and vary in size from 4  $\mu\text{m}$  at the inner margin of the shell to less than 1  $\mu\text{m}$  at the outer. In some instances where pyrite has pseudomorphed the prismatic layer of the original shell, no pyrite crystal form is discernible.

3. Pyritized internal moulds occur within most organic cavities:

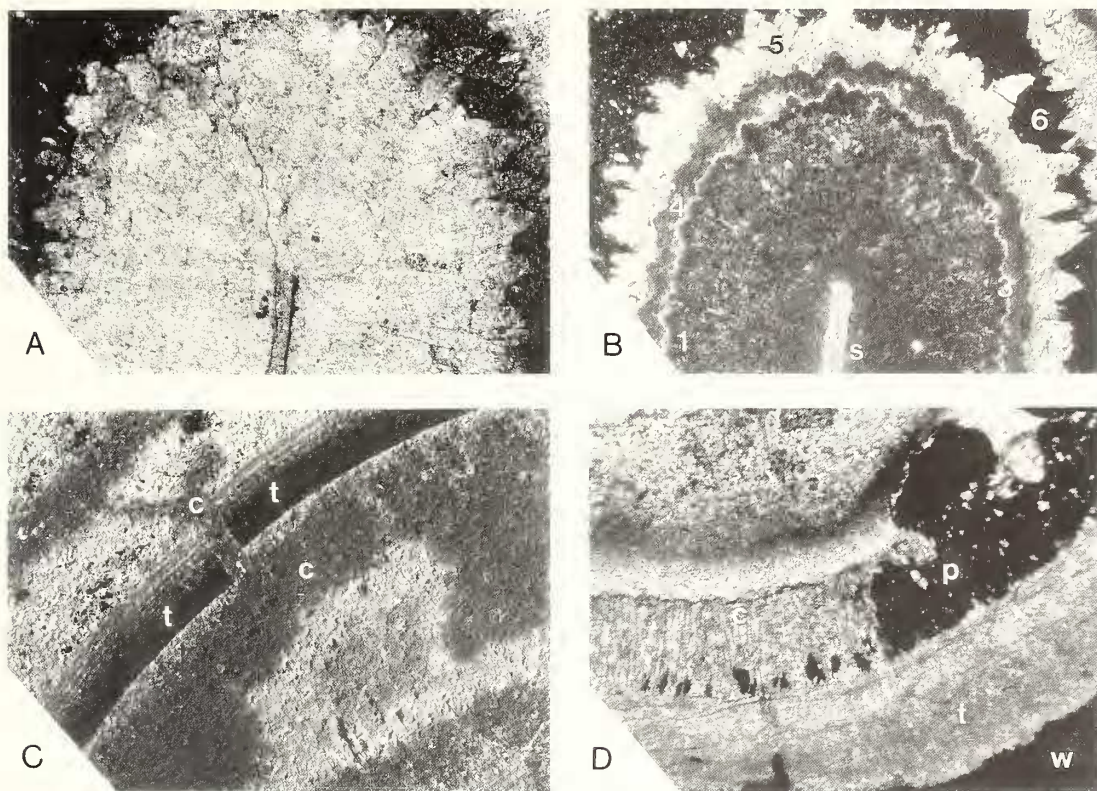
- a. Within calcified wood pyrite, framboids infill the large fluid bearing vessels (text-fig. 6C).
- b. Octahedral pyrite with a pore-lining habit occurs within the vesicles of spongy bone in vertebrae (text-fig. 6H).
- c. The internal cavities of gastropods contain geopetal pyritized sediment, and pyrite linings. In some cases the latter extend downwards from the upper surface of the cavity to form what Hudson (1982) referred to as pyrite stalactites (text-fig. 9B). The crystallites here adopt the octahedral habit and are between 40 and 100  $\mu\text{m}$  across.
- d. Within *Teredina* cavities, pyrite occurs as permineralized sediment and as a bore lining, the combination of both habits in the same cavity producing a geopetal structure (text-fig. 9F). In some cases the pyrite has obviously pseudomorphed calcareous linings within the *Teredina* borings (text-figs. 9E and 10D), although it also occurs as a discrete coat of crystallites dusting the surface of some calcified *Teredina* infills within pyritized wood. The crystals in this case adopt a octahedral habit and are generally less than 10  $\mu\text{m}$  in size.

4. Pyrite overgrowths, termed overpyrite by Hudson (1982), occur on the surface of most fossils. It adopts the following morphologies:

- a. Mineralized burrow traces occur on the surface of all fossil types. Octahedral crystallites are most common in the 40–100  $\mu\text{m}$  size range. In most cases the pyrite extends beyond the zone of burrowing onto the surface of the fossil.
- b. A light dusting of bipyramidal euhedral 40  $\mu\text{m}$  crystallites occurs on the surface of some eumalacostracan carapaces within phosphatic concretions (text-fig. 12E). The pyrite is limited to the surface of the fossil and is patchy in extent.
- c. Cauliform pyrite growths (Ramdohr 1980) upon the surface of fossils are frequently associated with pyritized trace fossils and show two forms of crystal habit.
  - i. Octahedral in the 40–100  $\mu\text{m}$  size range, identical to the 'light dusting' described above although better developed and forming an uneven cauliform coat.
  - ii. Radiating crystals producing a very smooth cauliform growth 1–2 cm across covered with euhedral cubic crystals 1–2 mm across (text-fig. 9C), although a vertical polished section through the growth reveals a radiating cone in cone crystal structure.

5. Pyrite concretions occur as flattened to sub-spherical concretions 1–10 cm across which in places coalesce to form an aggregated mass. In some specimens relict sediment is clearly visible





TEXT-FIG. 10. A, thin-section of syntaxial calcite overgrowths on *Teredina* fragment,  $\times 24$ . B, CL of A showing numbered luminescent calcite zones on shell fragment (c),  $\times 24$ . C, CL fractured *Teredina* calcite (t) that has been infilled with authigenic cavity-lining calcite (c),  $\times 36$ . D, thin section of bore-lining *Teredina* calcite (t) in wood (w); pore-lining calcite (c) syntaxial with *Teredina* calcite has been pseudomorphed by pyrite (p),  $\times 40$ .

and step-like striations along the horizontal axis of the nodule delineate original bedding. In hand specimens of this type the pyrite has a granular appearance. Alternatively, the pyrite adopts a cauliform growth habit. Horizontal sectioning of the concretions reveal a septarian fracture system of radial and concentric cracks infilled with euhedral pyrite. Septarian cracks formed as tensile fractures during burial and compaction of the host shale (Astin 1987). Pyrite septarian infills are limited to concretions of pyrite (described above) and calcium phosphate, and have not been recorded in carbonate concretions. Within the calcium phosphate concretions pyritization usually extends beyond the septarian fracture to replace phosphatized sediment.

*Paragenesis.* Of all the early diagenetic sedimentary minerals, pyrite has attracted the greatest interest through either geochemical studies of modern anaerobic systems or mineralogical studies of the geological occurrence (Berner 1970, 1971, 1984; Curtis 1980). Under anaerobic conditions, iron hydroxide within sediment pore waters is reduced during bacterial respiration to produce iron ions. Following the depletion of iron hydroxide, bacterial respiration utilizes the sulphate ion present in sea water forming hydrogen sulphide as a by-product. The subsequent reaction of these two reactive species leads to the formation of an initial iron monosulphide which upon further reaction with elemental sulphur forms pyrite.

The overall pyrite content of the London Clay is low. Burrowing organisms were probably able



to supply sufficient oxygen to the decomposition system to facilitate prolonged aerobic decay. Thus low concentrations of iron and sulphate ions were produced by anaerobic microbial reduction and pyrite formation was hindered. Pyrite was precipitated at several stages in the diagenetic history of the sequence (Table 1 and text-fig. 14). This sequence resembles that in pyrite-bearing shales from the Jurassic of England and Germany (Hudson 1982).

Pyrite framboids within concretions are morphologically identical to those dispersed in the sediment and were therefore the first pyrite phase to form. Framboid formation was concentrated at sites of active anaerobic decay such as decomposing plants and animals in response to bacterial decomposition and in some cases formed pyrite concretions and pyritized sediment infills of organic cavities.

Some gastropods have been crushed by sediment overburden prior to the formation of cavity lining pyrite and pyritized sediment infills. Others show no compaction cracks. This may be due to structural variation in the shells and/or a timing variation in pyrite formation. Overpyrite also formed at this time since it is contiguous with compaction fractures and internal pore-lining pyrite. Pyritization of plant remains is also likely to have occurred at this time since some of the pyritized plant remains have been partially flattened.

It is not possible to date the formation of some of the pyrite morphotypes, such as pyrite concretions relative to other mineral phases, because they do not occur in conjunction with other minerals or varieties of pyrite. However, concretion shape is strongly controlled by sediment porosity. If permeability is equal in both the horizontal and vertical planes then the concretions will tend to be spherical. After a degree of compaction sediment permeability is greatest in the horizontal plane and the concretions that form tend to be discoidal. Thus it is likely that the flattened pyrite concretions formed later than the more spherical forms.

Alteration of pyrite by calcium rich pore waters during weathering led to the formation of gypsum crystals (text-fig. 9C, D).

### *Calcite*

*Morphology.* Calcium carbonate within the London Clay occurs as original skeletal fragments and as mud-rock concretions. The latter form prominent bands of spherical to flattened ovate concretions along the foreshore and cliff exposures at Sheppey and are commonly in the 20–80 cm size range although some reach over 1 m in diameter. Fossils within the concretions include wood and occasional shelly debris and appear to be most common within one band along the foreshore. Elsewhere the majority of the concretions are unfossiliferous, although frequently intensively bioturbated, with burrows being most prominent on the outside of the concretion. Septaria are most common within non-fossiliferous concretions and are frequently filled with a green-yellow calcite with occasional selenite. The concretions are also associated with depositional events, e.g. the lowest nodule bank in the cliffs of Warden Point occurs in a dark blue-black band of clay which flames into the overlying bed.

Much of the wood within concretions has been intensively bored by *Teredina* and the borings have been infilled with geopetal sediment and calcite (text-fig. 5B, C). At least four colour zones are visible in hand specimen in the calcite lining the borings (text-fig. 5C). Differences in chemical composition of the calcite, particularly in manganese levels, render it amenable to cathodoluminescence microscopy (CL). CL clearly shows six dullish red zones (text-fig. 10) coating shell fragments and *Teredina*-calcite lining the borings. The bore-lining calcite is brighter, indicating a higher manganese/iron ratio, whereas the dull red pore-lining calcite is indicative of a lower manganese/iron ratio. The initial phase of pore-lining calcite is frequently syntaxial with skeletal fragments and adopts a radial habit, whereas later zones are typically sparry.

*Chemistry.* Both chemical analysis and original porosity determinations (Table 2) show a series of clear trends between the rim and core of the concretion.

The decrease in porosity away from the centre of the concretion reflects the timing of mineral formation. At the centre of the nodule carbonates were precipitated prior to appreciable sediment

TABLE 2. Chemical analysis of pyrite, phosphate, and calcite concretions.

	Phosphate concretion				Calcareous concretion			
	P <sub>1</sub> Core	P <sub>2</sub>	P <sub>3</sub>	P <sub>4</sub> Rim	C <sub>1</sub> Core	C <sub>2</sub>	C <sub>3</sub>	C <sub>4</sub> Rim
Ca (%)	40.8	34.2	39.7	36.7	35.7	33.3	30.2	31.4
Fe (%)	3.72	5.19	4.68	4.53	3.74	3.93	3.65	4.49
Mn (ppm)	888	734	656	540	7007	6880	5720	4063
Mg (%)	0.50	0.48	0.49	0.49	1.40	1.40	1.42	1.54
Al (%)	1.66	1.64	1.59	1.58	2.58	2.79	2.91	4.36
P (%)	35.8	28.2	34.3	25.8	2.34	2.54	1.97	2.21
Si (%)	9.8	11.3	12.4	23.8	14.5	15.7	14.9	27.6
Mn/Ca	0.0021	0.0021	0.0016	0.014	0.19	0.20	0.18	0.12
Internal porosity (%)	82	78	76	54	72.1	73.7	68.8	54.7
	(estimated from Si and Al content)				(acid soluble fraction)			

compaction. Later phases of mineral growth occurred after the onset of compaction and consequent reduction of sediment porosity. The decreasing calcium and increasing aluminium (from detrital clay minerals) levels towards the rim of the nodule are a function of this control on growth. The depletion of manganese away from the centre of the nodule is also partly a function of original porosity, since the manganese occurs as a carbonate with the calcite. However, the manganese/calcium ratio at the rim of the concretion is 35% lower than at the core.

*Paragenesis.* The high internal porosities (between 80–90%) recorded within calcite concretions indicate an early diagenetic origin. Porosities of this value within mud rocks only occur within the top 5 m of sediment (Greensmith 1978). Such an early diagenetic origin has been attributed by Berner (1968) and Raiswell (1971, 1976) to the bacterial degradation of organic matter.

Berner (1968) showed experimentally that calcium may be concentrated as calcium stearate (a soap) within the alkaline decay aureole of proteinaceous animals. Stearate is the stable calcium salt in this case and Berner suggested that calcite may form following its depletion. The formation of calcite would be promoted by a high pH microenvironment generated by the production of ammonia from putrefying proteins. In the London Clay soft parts were scavenged and decomposed prior to mineralization. An alternative process must therefore have been responsible for the formation of the calcareous concretions.

In a marine environment, sediment pore waters achieve a high level of calcium saturation. The precipitation of a calcareous mineral phase is therefore controlled by anionic concentration gradients. Bicarbonate ions produced during anaerobic decay may react with the calcium ion to form calcite (Raiswell 1971, 1976). Bicarbonate ion concentration may be centred around discrete pockets of decomposing organic matter (e.g. megafossils) or within whole beds of organic rich sediment.

The occurrence of discrete layers of concretions and the dearth of contained fossils suggests that the bicarbonate ions originated from the decomposition of disseminated organic carbon in the London Clay. Further, the occurrence of concretion bearing horizons within flamed beds suggests a depositional control upon nodule formation. Rapid burial of an organic-rich layer of sediment would lead to anoxia and the production of large amounts of the bicarbonate ion, thereby promoting carbonate formation. The irregular development of discontinuous bands of concretions in the London Clay may therefore represent episodic burial events.

The introduction of manganese into the calcite lattice is due to microbial respiration within sediment. Manganese reduction is the highest reduction zone in the sediment pile and occurs in

the poorly oxygenated sediments below the sediment-water interface. Manganese ions liberated by microbial respiration become concentrated within sediment pore waters and may, upon reaction with bacterially produced anionic species, e.g. the bicarbonate ion, precipitate as a mineral phase. In the London Clay manganous mineral species were incorporated into other mineral precipitates such as calcite and phosphate. About 0.75% of manganese occurs within the carbonate fraction of the concretions. This is because initial stages of concretion growth occurred at or near the zone of manganese reduction which provided an abundant source of manganese ions for inclusion into the calcite lattice. The reduced levels of manganese towards the rim of the concretion show that this part of the nodule formed deeper in the sediment pile when ionic manganese within sediment pore waters was depleted.

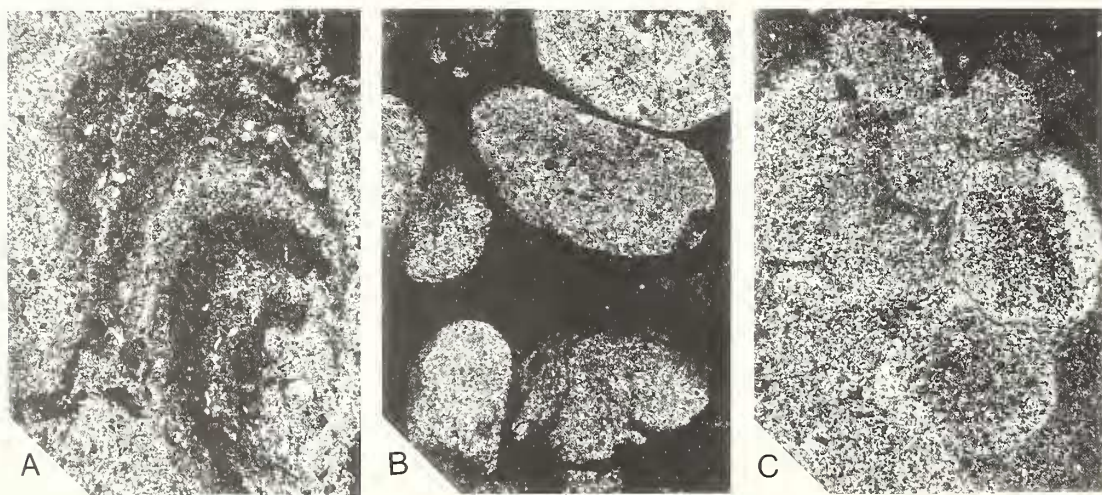
Thin-section CL of wood-bearing concretions shows that the wood luminesces at the same intensity as the surrounding sediment. Since CL is sensitive to changes in manganese and iron chemistry this shows that levels of these elements within the wood and surrounding concretion are the same. Calcification of wood within the London Clay is therefore an early event and synchronous with the early stages of concretion growth.

The development of pore-lining calcite in some *Teredina* borings occurred after sediment infill and either during or after the development of calcareous concretions. Septarian cracks formed during burial at a depth of up to 50 m (Astin 1987).

### *Calcium phosphate*

**Morphology.** King (1981) documented bands of phosphatic concretions at Sheppey although they are more commonly randomly dispersed. XRD shows the phosphate to be francolite, a calcium fluor-apatite, which occurs in the form of 1–2  $\mu\text{m}$  sized crystal aggregates. The concretions are ovate and up to 60 cm in size. They are a light buff colour in contrast to the dark brown-black fossil material which they occasionally contain. Organic remains in the concretions includes faecal pellets, burrows and fragments of arthropods and vertebrates (text-fig. 11A, C). The fossils are composed of francolite virtually identical to that forming the surrounding concretion, apart from a slight deviation in minor element chemistry. The colour difference between fossils and the enclosing concretion is probably a function of crystal size.

Most of the fossils encountered in phosphatic concretions had an original phosphate component.



TEXT-FIG. 11. Thin section of phosphate concretions. A, burrows with spreite structure,  $\times 18$ . B, faecal pellets surrounded by pyrite,  $\times 25$ . C, faecal pellets with pyrite veining,  $\times 20$ .

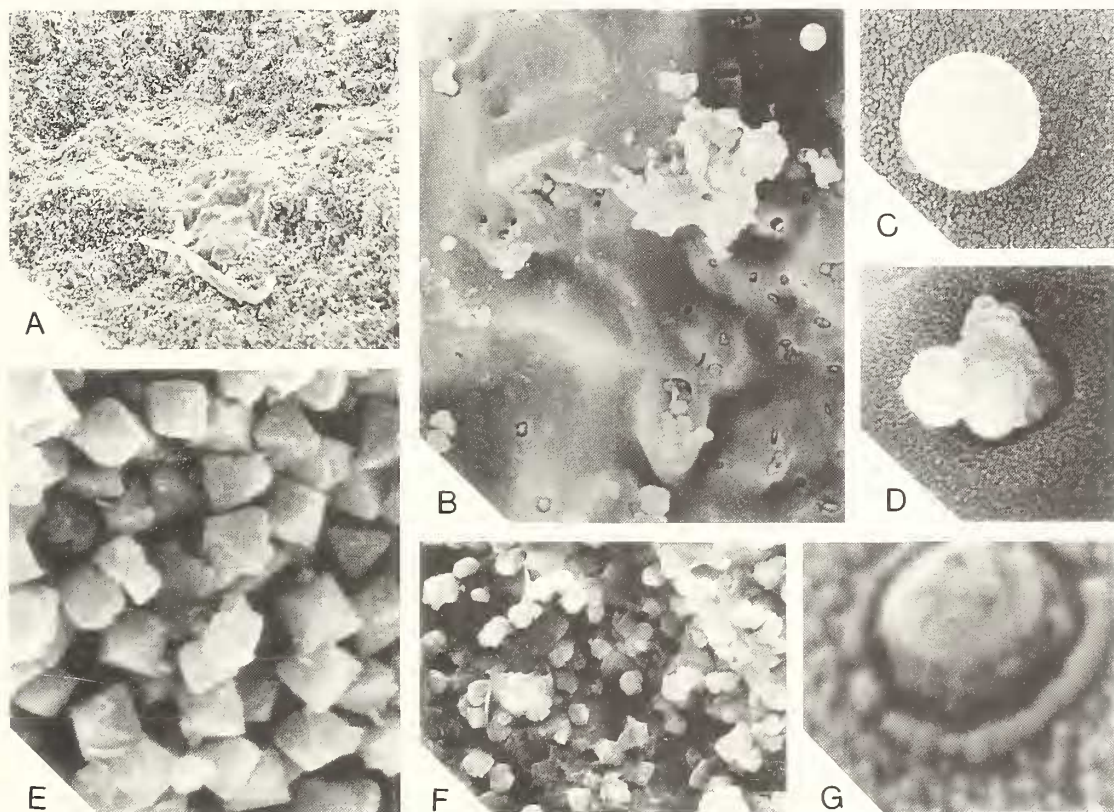


However, in the case of the arthropod cuticle this was probably quite low since phosphate content of living arthropod cuticle is in the region of 1–5% dry weight (Allison 1988a). Non-concretionary phosphate is limited to isolated fish teeth which are most commonly encountered in the coarse sands near the base of the cliff and may have originated from eroded concretions.

**Chemistry.** Original porosities were estimated by chemical analysis. Manganese levels and the calcium/manganese ratio decrease towards the rim of the concretion (Table 2). Internal porosities are slightly higher than those of carbonate concretions although the difference may be within experimental error.

**Paragenesis.** Phosphate mineralization occurred after the formation of framboidal pyrite but before pyritization of *Nipa* and some shelly fossils, and before the formation of flattened concretions. This is evidenced by the presence of high internal porosities, by pyrite framboids in the concretions, and by three-dimensional preservation of fruits and gastropods in phosphate concretions but not in pyrite concretions.

In normal marine pore waters, concentrations of the bicarbonate ion exceed those of phosphate (Gulbrandsen 1969) and the most stable calcium mineral phase is normally calcite. Pore-water phosphate levels must therefore be considerably enriched to allow the precipitation of phosphate minerals. Gulbrandsen (1969) suggested that such enrichment may result from the bacterial



TEXT-FIG. 12. SEMs of crab-bearing nodule. A, fine mass of phosphate crystallites with organic pockets,  $\times 80$ . B, smooth organic pocket with small phosphate crystallites,  $\times 8000$ . C, 'bacterial' microsphere,  $\times 18\,000$ . D, aggregated microspheres,  $\times 10\,000$ . E, octahedral pyrite upon surface of crab,  $\times 7000$ . F, phosphate crystallites,  $\times 3800$ . G, 'bacterial' microsphere with possible cell wall,  $\times 38\,000$ .

degradation of organic matter such as marine plankton. Further, Lucas and Prévôt (1984) have shown experimentally that phosphate can be liberated by the microbial breakdown of organic compounds such as adenosine-tri-phosphate (ATP), used by most organisms for energy transfer. Benmore *et al.* (1983) believe that phosphate liberated in this way would become adsorbed to ferric hydroxides in aerobic sediment. Under anaerobic conditions these iron compounds would be reduced and phosphate would be liberated into solution. Thus phosphate concentrations at the anoxic-oxic boundary may be sufficiently increased to allow localized phosphate precipitation.

Phosphate precipitation may also be induced by bacteria, e.g. plaque bacteria precipitate apatite crystals inside the cell when phosphate concentrations are high. Ennever *et al.* (1981) showed that several strains of bacteria can phosphatize in this way when cultured in the correct medium. Further, phosphate crystalites from London Clay concretions are generally rounded bacteria-sized crystalline aggregates about 1–2  $\mu\text{m}$  in diameter (text-fig. 12A, D, G). In some cases the crystalites are enclosed (text-fig. 12G) by what appears to be the cell wall of the bacterium. It is therefore a possibility that these microspherical crystalites may be a bacterial precipitate formed at the anoxic-oxic interface where phosphate concentrations are high. However, such a microspherical form could also be a product of physico-chemical conditions, e.g. rapid precipitation around a multitude of nuclei from a saturated solution could produce a similar crystal form.

Manganese concentrations at the outer edge of the concretions are much lower than at the centre of the nodule (Table 2). This is because pore-water manganese levels were lower during this late stage of growth. This depletion is considered to be due to bacterial manganese reduction, as documented above (p. 1094), but it is not meaningful to compare manganese levels in phosphate and calcite concretions, since each mineral has a different affinity for the element.

Many fossils in the phosphate concretions have been replaced by secondary francolite. It is not possible to date this mineralization relative to the formation of the concretions. Lucas and Prévôt (1984) showed experimentally that phosphatization of calcareous skeletal material may occur rapidly if pore-water phosphate levels are high enough.

In the London Clay, phosphatization of fossils appears to be restricted to organic remains with an original phosphate content (Balson 1980) e.g. arthropods, vertebrates, and faecal pellets.

## SUMMARY

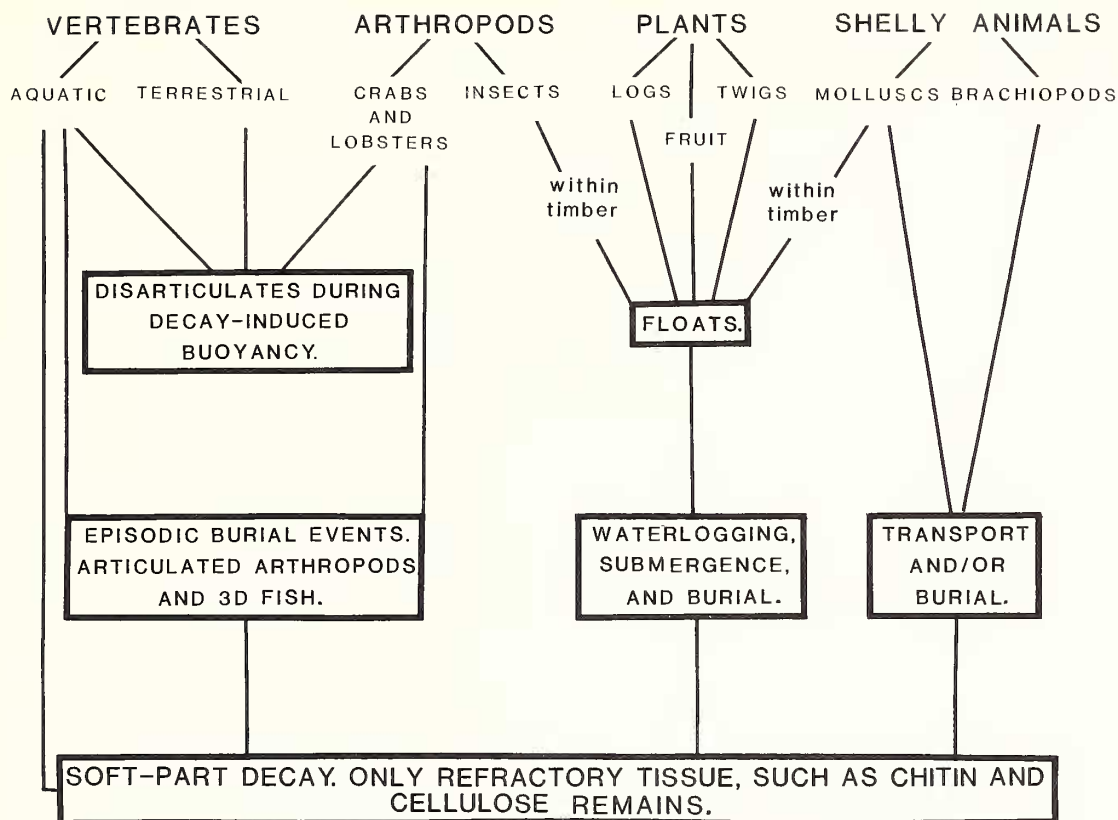
The Eocene London Clay cropping out on the Isle of Sheppey contains a suite of early diagenetic calcareous, phosphatic, and pyrite concretionary growths which are often fossiliferous (see text-figs. 13 and 14 for diagenetic and taphonomic summary). Framboidal pyrite formed first in small anaerobic pockets in an otherwise aerobic and bioturbated sediment. The bacterial decomposition of organic matter in this aerobic zone liberated phosphate into pore-water solutions which became adsorbed to ferric hydroxides in the sediment (Benmore *et al.* 1983). The reduction of iron at the anoxic-oxic interface liberated phosphate into solution which was precipitated either abiotically or by sediment bacteria to form small concretionary bodies around faecal pellets, burrows, arthropods, and vertebrates. Phosphatization was specific to organisms with an original phosphatic content.

Calcareous concretions formed as a result of rapid burial of organic rich layers. Subsequent anaerobic decay of the organic matter in these layers promoted an increase in pore-water concentrations of the bicarbonate ion which led to the precipitation of calcium carbonate. Precipitation occurred around sediment inhomogeneities and megafossils which may have functioned as 'seed crystals'.

Framboidal pyrite formed internal moulds in some organic cavities and laminated cauliform concretions. Pyritic replacement of organic remains, such as shelly fossils and plant material, occurred later in the diagenetic sequence after sediment compaction.

Concretionary phosphate was clearly the earliest preservational mineral to form in the London Clay. Mineralization is the principal means of halting the information loss that occurs during decay (Allison 1988a, b). Therefore organisms preserved during the first stages of the diagenetic





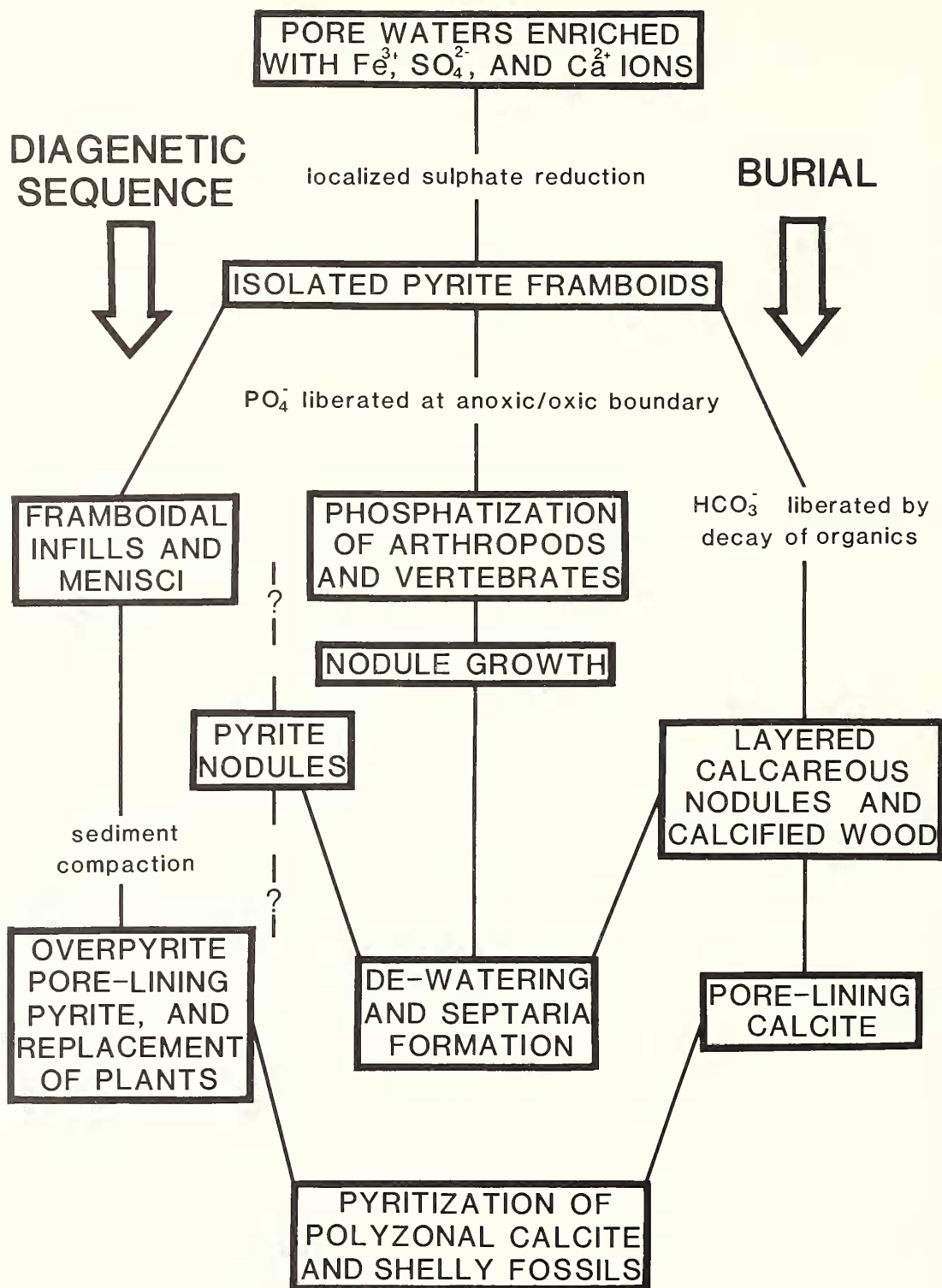
TEXT-FIG. 13. Summary of biostratinomic sequence.

sequence exhibit a higher level of preservation than those mineralized later. Since phosphatization can be restricted to taxonomic groups with an original phosphate content a diagenetic taphonomic bias is seen to function.

From the recognition of this preservational bias and a knowledge of the geochemical switches governing mineral precipitation it is possible to characterize the conditions necessary for exceptional preservation and apply them to the fossil record. With further work it will also be possible to predict the level of preservation which can be expected in a given sedimentary regime.

Since early diagenetic minerals are strongly indicative of depositional environment they can be considered as mineralogical taphofacies (Brett and Baird 1986). Thus the phosphatic taphofacies is commonly associated with the highest levels of fossil preservation (Allison 1988b). For example, the highest level of fossil preservation is that of three-dimensional muscle-fibres. Such fossils are more commonly encountered preserved in phosphate than any other mineral form (e.g. Cretaceous fish from Brazil, Martill 1988; ichthyosaurs from the Jurassic of the English Midlands, Martill 1987; and the mantle of squid from the Jurassic of south-west England, Donovan 1983; Allison 1988c).

*Acknowledgements.* Dr D. E. G. Briggs provided guidance for this work and together with Dr J. D. Hudson critically reviewed an earlier draft of the manuscript. Drs V. P. Wright, E. N. K. Clarkson, and D. M. Martill also commented on various aspects of this work. I am especially appreciative of the guidance provided by A. J. Kemp of Bristol on geochemical analysis. Joyce Smith at Friday Harbor kindly entered the text into a word processor and Dr M. E. Collinson discussed aspects of the biology of *Nipa burtini* and kindly donated



TEXT-FIG. 14. Summary of diagenetic sequence.



several specimens. I am also grateful to R. Gutterie of Wells Kauff Kramer for taking the X-ray radiographs of the phosphate concretions. This work was carried out during the tenure of a NERC award at the University of Bristol and completed during the tenure of a Friday Harbor Post-Doctoral Fellowship at the University of Washington, USA.

## REFERENCES

- ALLISON, P. A. 1988a. The role of anoxia in the decay and mineralization of proteinaceous macrofossils. *Paleobiology*, **14**, 139–154.
- 1988b. *Konservat-Lagerstätten*: cause and classification. *Ibid.* In press.
- 1988c. Phosphatized soft-bodied squid from the Jurassic Oxford Clay. *Lethaia*, **21**, 293–301.
- ASTIN, T. R. 1987. Septarian crack formation in carbonate concretions from shales and mudstones. *Clay Miner. Bull.* **21**, 617–631.
- BALSON, P. S. 1980. The origin and evolution of Tertiary phosphorites from eastern England. *J. geol. Soc. Lond.* **137**, 723–729.
- BENMORE, R. A., COLEMAN, M. L. and MCARTHUR, J. M. 1983. Origin of sedimentary francolite from its sulphur and carbon isotope composition. *Nature, Lond.* **302**, 516–518.
- BERNER, R. A. 1968. Calcium carbonate concretions formed by the decomposition of organic matter. *Science, NY*, **159**, 195–197.
- 1970. Sedimentary pyrite formation. *Am. J. Sci.* **268**, 1–23.
- 1971. *Principles of chemical sedimentology*, 240 pp. McGraw Hill, New York.
- 1981. Authigenic mineral formation resulting from organic matter decomposition in modern sediments. *Fortschr. Miner.* **59**, 117–135.
- 1984. Sedimentary pyrite, an update. *Geochim. Cosmochim. Acta*, **48**, 605–615.
- BRETT, C. E. and BAIRD, G. C. 1986. Comparative taphonomy: a guide to paleoenvironmental interpretation based on fossil preservation. *Palaios*, **1**, 207–227.
- BRIGGS, D. E. G. and WILLIAMS, S. H. 1981. The restoration of flattened fossils. *Lethaia*, **14**, 157–164.
- CASIER, E. 1966. *Faune Ichthyologique du London Clay*, 496 pp. British Museum (Natural History), London.
- CHANDLER, M. E. J. 1961. *The Lower Tertiary Floras of Southern England. I Palaeocene Floras. London Clay Flora (supplement). Text and Atlas*. 354 pp. British Museum (Natural History), London.
- 1964. *The Lower Tertiary Floras of Southern England IV. A survey of findings in the light of recent botanical observations*. 151 pp. British Museum (Natural History), London.
- COLLINSON, M. E. 1983. *Fossil plants of the London Clay: Palaeontological Association field guide to fossils 1*, 121 pp., Palaeontological Association, London.
- CONWAY MORRIS, S. 1979. Middle Cambrian polychaetes from the Burgess Shale of British Columbia. *Phil. Trans. R. Soc.* **B285**, 227–274.
- CURRY, D. 1965. The English Palaeogene pteropods. *Proc. malac. Soc. Lond.* **36**, 357–371.
- CURTIS, C. D. 1980. Diagenetic alteration in black shales. *J. geol. Soc. Lond.* **137**, 189–194.
- DAVIS, A. G. 1936. The London Clay of Sheppey and the location of its fossils. *Proc. geol. Ass.* **47**, 328–345.
- and ELLIOT, G. F. 1957. The palaeogeography of the London Clay sea. *Ibid.* **68**, 255–277.
- DONOVAN, D. T. 1983. *Mastigophora* Owen 1856: a little-known genus of Jurassic coleoids. *Neues Jb. Geol. Paläont. Abh.* **165**, 484–495.
- ENNEVER, J., STRECKFUSS, J. L. and GOLDSCHMIDT, M. C. 1981. Calcifiability comparison among selected micro-organisms. *J. Dent. Res.* **60**, 1793–1796.
- GILKES, R. J. 1967. Clay Mineral provinces in the Tertiary sediments of the Hampshire Basin. *Clay Minerals*, **7**, 351–361.
- GREENSMITH, J. T. 1978. *Petrology of the sedimentary rocks*. 241 pp. Allen & Unwin, London.
- GULBRANDSEN, R. A. 1969. Physical and chemical factors in the formation of marine apatite. *Econ. Geol.* **64**, 365–382.
- HARRISON, C. J. O. and WALKER, C. A. 1977. Birds of the British Lower Eocene. *Tert. Res. Spec. Pap.* **3**, 1–96.
- HOOKE, J. J., INSOLE, A. N., MOODY, R. J. J., WALKDEN, C. A. and WARD, D. A. 1980. The distribution of cartilaginous fish, turtles, birds and mammals in the British Palaeocene. *Tert. Res.* **3**, 1–45.
- HUDSON, J. D. 1982. Pyrite in the ammonite bearing clays from the Jurassic of England and Germany. *Sedimentology*, **29**, 639–667.
- KEEN, M. C. 1978. The Tertiary-Palaeogene. In BATE, R. and ROBINSON, E. (eds.). *A Stratigraphical Atlas of the British Ostracoda*, 385–450. Seel House Press, London.

- KENRICK, P. and EDWARDS, D. 1988. The anatomy of Lower Devonian *Gosslingia breconensis* Heard based upon pyritized axes, with some comments on the permineralization process. *Bot. J. Linn. Soc.* **97**, 95–123.
- KING, C. 1981. The stratigraphy of the London Clay and associated deposits. *Tert. Res. Spec. Pap.* **6**, 1–158.
- and KING, A. D. 1976. A London Clay section at Waterworks Corner, Woodford, Essex. *Tert. Res.* **1**, 21–24.
- KNOX, R. W. O'B. and HARLAND, R. 1979. Stratigraphical relationships of the Early Palaeogene Ash Series of N.W. Europe. *J. geol. Soc. Lond.* **136**, 463–470.
- LUCAS, J. and PRÉVÔT, L. 1984. Apatite synthesis by bacterial activity from phosphatic organic matter and several calcium carbonates in natural fresh water and seawater. *Chem. Geol.* **42**, 101–118. [In French.]
- MARTILL, D. M. 1987. A taphonomic and diagenetic case study of a partially articulated ichthyosaur. *Palaeontology*, **30**, 543–555.
- 1988. The preservation of fishes in concretions from the Santana Formation (Cretaceous) of Brazil. *Ibid.* **31**, 1–18.
- MURRAY, J. W. and WRIGHT, C. A. 1974. Palaeogene foraminiferida and palaeoecology, Hampshire and Paris Basins and the English Channel. *Spec. Pap. Palaeont.* **14**, 171 pp.
- QUAYLE, W. J. and COLLINS, J. S. 1981. New Eocene crabs from the Hampshire Basin. *Palaeontology*, **24**, 733–758.
- RAMDOHR, P. 1980. *The ore minerals and their intergrowths* (2nd edn.), 1202 pp. Pergamon, Oxford.
- RAISWELL, R. 1971. The growth of Cambrian and Liassic concretions. *Sedimentology*, **17**, 147–171.
- 1976. The microbiological formation of carbonate concretions in the Upper Lias of N.E. England. *Chem. Geol.* **18**, 227–244.
- REDFIELD, A. C. 1958. The biological control of chemical factors in the environment. *Am. Scient.* **46**, 206–226.
- ROWELL, A. J. and RUNDLE, A. J. 1967. Lophophore of the Eocene Brachiopod *Terebratulina wardenensis*, Elliot. *Paleont. Contr. Univ. Kans. Paper* **15**, 18 pp.
- RUNDLE, A. J. and COOPER, J. 1970. Occurrence of a fossil insect larva from the London Clay of Herne Bay, Kent. *Proc. geol. Ass.* **82**, 239–296.
- SEILACHER, A. 1970. Begriff und Bedeutung der Fossil-Lagerstätten. *Neues Jb. Geol. Paläont. Abh.* **1970**, 34–39.
- REIF, W. E. and WESTPHAL, F. 1985. Sedimentological, ecological and temporal patterns of fossil Lagerstätten. *Phil. Trans. R. Soc. Lond.* **B311**, 5–23.
- VENABLES, E. M. and TAYLOR, H. E. 1963. An insect fauna of the London Clay. *Proc. geol. Ass.* **73**, 273–279.
- WARD, D. J. 1979. Additions to the fish fauna of the English Palaeogene. I. Two specimens of *Aliopas* (thresher shark) from the English Eocene. *Tert. Res.* **2**, 23–28.
- WILLS, L. J. 1951. *A palaeogeographical atlas of the British Isles and adjacent parts of Europe*, 114 pp. Blackie, London.
- WILKINSON, H. P. 1983. Starch grain casts and moulds in Eocene (Tertiary) fossil mangrove hypocotyls. *Ann. Bot.* **51**, 39–45.
- ZANGERL, R. 1971. On the geologic significance of perfectly preserved fossils. *Proc. First North Am. Paleont. Conv.* **1**, 1207–1222.
- and RICHARDSON, E. S. 1963. The paleoecological history of two Pennsylvanian black shales. *Fieldiana, Geol. Mem.* **4**, 1–352.

PETER A. ALLISON

Friday Harbor Laboratories  
University of Washington  
620 University Road  
Friday Harbor  
Washington 98250, USA

Typescript received 24 April 1987

Revised typescript received 3 May 1988